Human Molecular Genetics, 2015, Vol. 24, No. 3 **787–801**
doi:10.1093/hmg/ddu497
Advance Access published on September 25, 2014

Activation of AMP-activated protein kinase α1 mediates mislocalization of TDP-43 in amyotrophic lateral sclerosis

Yu-Ju Liu[1,2], Tz-Chuen Ju[2], Hui-Mei Chen[2], Yu-Sung Jang[2], Li-Ming Lee[3], Hsing-Lin Lai[2], Hua-Chia Tai[4], Jim-Min Fang[4], Yun-Lian Lin[5], Pang-Hsien Tu[2,*] and Yijuang Chern[1,2,5,*]

[1]Graduate Institute of Life Sciences, National Defense Medical Center, Taipei, Taiwan, [2]Division of Neuroscience, Institute of Biomedical Sciences, Academia Sinica, Taipei, Taiwan, [3]Institute of Neuroscience, National Yang-Ming University, Taipei 112, Taiwan, [4]Department of Chemistry, National Taiwan University, Taipei 106, Taiwan and [5]National Research Institute of Chinese Medicine, Taipei 112, Taiwan

Received July 23, 2014; Revised September 8, 2014; Accepted September 22, 2014

TAR DNA-binding protein-43 (TDP-43) is a nuclear RNA-binding protein involved in many cellular pathways. TDP-43-positive inclusions are a hallmark of amyotrophic lateral sclerosis (ALS). The major clinical presentation of ALS is muscle weakness due to the degeneration of motor neurons. Mislocalization of TDP-43 from the nucleus to the cytoplasm is an early event of ALS. In this study, we demonstrate that cytoplasmic mislocalization of TDP-43 was accompanied by increased activation of AMP-activated protein kinase (AMPK) in motor neurons of ALS patients. The activation of AMPK in a motor neuron cell line (NSC34) or mouse spinal cords induced the mislocalization of TDP-43, recapitulating this characteristic of ALS. Down-regulation of AMPK-α1 or exogenous expression of a dominant-negative AMPK-α1 mutant reduced TDP-43 mislocalization. Suppression of AMPK activity using cAMP-simulating agents rescued the mislocalization of TDP-43 in NSC34 cells and delayed disease progression in TDP-43 transgenic mice. Our findings demonstrate that activation of AMPK-α1 plays a critical role in TDP-43 mislocalization and the development of ALS; thus, AMPK-α1 may be a potential drug target for this devastating disease.

INTRODUCTION

Amyotrophic lateral sclerosis (ALS) patients develop muscle weakness and impaired voluntary movement, which are caused by the degeneration of motor neurons (1). TAR-DNA-binding protein-43 (TDP-43)-positive inclusions in the brain and the spinal cord are a hallmark of ALS (2). Although ∼95% of ALS patients suffer from sporadic ALS without family history (3,4), mutations of a handful of genes were discovered in familial ALS patients and a subset of sporadic ALS patients. Therefore, the genetic contribution of dominant mutations with low penetrance to ALS might be higher than what has been recognized (5). Environmental exposure to risk factors that have yet to be clearly identified also plays critical roles in the development of ALS (6). Several drugs (e.g. Riluzole, Lioresol®, Zanaflex® and non-steroidal anti-inflammatory drugs) are currently available and are frequently used for the treatment of ALS. Nonetheless, these drugs are non-specific and exert only limited effects (7).

The signature protein of ALS, TDP-43, is a nuclear protein consisting of 414 amino acids. Accumulating evidence demonstrates that TDP-43 functions in a wide variety of important cellular pathways, including gene regulation, pre-mRNA processing, microRNA expression and neuronal activity (8–10). In addition to the formation of TDP-43 inclusions, mislocalization of TDP-43 from the nucleus to the cytoplasm has been recognized as an early event of ALS that may cause detrimental effects (11). Because cytoplasmic TDP-43 inclusions are typically accompanied by nuclear clearance of TDP-43, ALS pathogenesis may, at least partially, be attributed to the loss of the nuclear functions of TDP-43 (12). Once excluded from the nucleus, the mislocalized TDP-43 in the cytoplasmic compartment can be degraded via autophagy and the proteasome (13). Arguably,

*To whom correspondence should be addressed at: Institute of Biomedical Sciences, Academia Sinica, Nankang, Taipei 115, Taiwan. Tel: +886 226523913; Fax: +886 227829143; Email: bmychern@ibms.sinica.edu.tw (Y.C.); Tel: +886 226523532; Fax: +886 227829143; Email: btu@ibms.sinica.edu.tw (P.-H.T.)

insufficient clearance of TDP-43 leads to the formation of TDP-43 inclusions. To date, the pathogenesis of TDP-43 mislocalization remains as a subject of intense examination.

Elevated oxidative stress has been widely detected in neurodegenerative diseases, including ALS (14), and is believed to contribute to the pathogenesis of sporadic ALS (15). It is not surprising that the onset and progression of ALS correlates well with the level of reactive oxygen species (ROS) in both mice and patients suffering from ALS (14,16). Previously, oxidative stress was demonstrated to regulate the nuclear cytoplasmic shuttling of some proteins (17,18). This finding is important because several transport factors [e.g. importin-α, cellular apoptosis susceptibility protein (CAS), Nup153, and NuP88] are sensitive to oxidative stress with respect to their localization, which in turn affects the nuclear transport of many proteins (19). Potential mechanisms that could mediate the activity of ROS described above include direct oxidation, posttranslational modifications and degradation of these transport factors. For example, phosphorylation of a nuclear transport factor (i.e. Nup50) by extracellular signal-regulated protein kinase/mitogen-activated protein kinase is known to alter its interaction with importin-β and subsequently leads to changes in nucleoporin-mediated nuclear transport (20). Consistent with the importance of ROS in nuclear cytoplasmic shuttling, Ayala and colleagues reported that oxidative stress-induced TDP-43 mislocalization (21). The underlying mechanism by which ROS alters the cellular localization of TDP-43 is currently unknown.

AMP-activated protein kinase (AMPK) is a major energy sensor that maintains cellular energy homeostasis (22). AMPK is a Ser/Thr kinase that stimulates pathways that promote energy production or inhibit energy expenditure (23). AMPK contains three subunits (α, β and γ) (23). The α subunit of AMPK is the catalytic subunit, and there are two different isoforms (α1 and α2). Recent studies revealed that AMPK could be directly activated by many upstream kinases, such as liver kinase B1 and calmodulin-dependent protein kinase kinase via phosphorylation of threonine^{172} within the catalytic domain of the α subunit. ROS is also known to regulate AMPK in a complex manner (24). The role of AMPK in ALS is of great interest because a recent study demonstrated that reduction in the activity of AMPK is beneficial in several genetic ALS models (25), but the underlying mechanism is currently unknown. In the present study, we demonstrate that abnormal activation of AMPK was closely associated with TDP-43 mislocalization in a motor neuron cell line (NSC34) and in the spinal cord of ALS patients. When triggered by elevated ROS, AMPK caused TDP-43 mislocalization and neuronal toxicity. Activation of the A_{2A} adenosine receptor ($A_{2A}R$) suppressed AMPK activation and rescued TDP-43 mislocalization via a cAMP/protein kinase A (PKA)-dependent pathway.

RESULTS

Aberrant activation of AMPK is associated with the mislocalization of TDP-43

AMPK has been implicated in several neurodegenerative diseases (24,26,27). A recent study demonstrated that a reduction of AMPK activity was beneficial in an ALS mouse model (mSOD1) (25). To evaluate the involvement of AMPK in patients suffering from ALS, we first determined the activity of AMPK based on the phosphorylation of threonine^{172} in AMPK-α (AMPK-α-p) in the choline acetyltransferase (ChAT)-positive motor neurons of ALS patients via immunohistochemical staining (28). Enhanced AMPK activation/phosphorylation was observed in ALS samples, but not in non-ALS controls, and intriguingly, closely correlated with the cytoplasmic mislocalization of TDP-43 in the motor neurons of all seven ALS cases examined (Table 1; Fig. 1; Supplementary Material, Fig. S1).

To explore the role of AMPK in TDP-43 mislocalization, a motor neuron-like cell line (NSC34) was treated with AICAR (1 mM for 24 h), an AMPK activator (29). Consistent with the finding in ALS patients, activation of AMPK caused the cytoplasmic mislocalization of TDP-43 based on immunocytochemical staining (Fig. 2A and B) and biochemical fractionation (Fig. 2C and D). Interestingly, treatment with AICAR (1 mM for 24 h) reduced the stability of TDP-43 protein 1 h after cycloheximide treatment (Fig. 2E and F). In addition, consistent with the results found in NSC34 cells, intrathecal injection of AICAR into the spinal cord of wild-type (WT) B6 mice for 24 h similarly triggered the cytoplasmic mislocalization of TDP-43 (Fig. 2G and H; Supplementary Material, Fig. S2). To further validate

Table 1. Summary of the demographic data, the neuropathology and the experimental results of the human subjects

Case	Age (year)	Section area	PMI (h)	Sex	AMPK activation (in motor neurons)	TDP-43 mislocalizatiom (in motor neurons)
ALS-1	49	Spinal cord	9	M	+++	+++
ALS-2	73	Spinal cord	10	F	+++	+++
ALS-3	61	Spinal cord	8	M	+++	++
ALS-4	58	Spinal cord	6	F	+++	+++
ALS-5	59	Spinal cord	6	M	+++	++
ALS-6	66	Spinal cord	6	F	+++	++
ALS-7	62	Spinal cord	9	F	+++	++
Non-ALS-1	42	Spinal cord	4	F	−	−
Non-ALS-2	45	Spinal cord	17	M	−	−
Non-ALS-3	73	Motor cortex	21	M	−	−

Significant levels of phosphorylated AMPK-α at Thr^{172} (AMPK-α-p) and cytosolic TDP-43 (Fig. 1) were detected in the ChAT-positive motor neurons in the ALS patients, but not in those of controls. Human sections were analyzed via immunofluorescence staining of AMPK-α-p, TDP-43 and ChAT, as shown in Figure 1 and Supplementary Material, Figure S1. The 4–12 ChAT-positive neurons were scored from 5 to 6 sections of each subject. PMI, postmortem interval. +++, 100% of the scored cells were positive; ++, ≥80% of the scored cells were positive; −, no positive cell was detected.

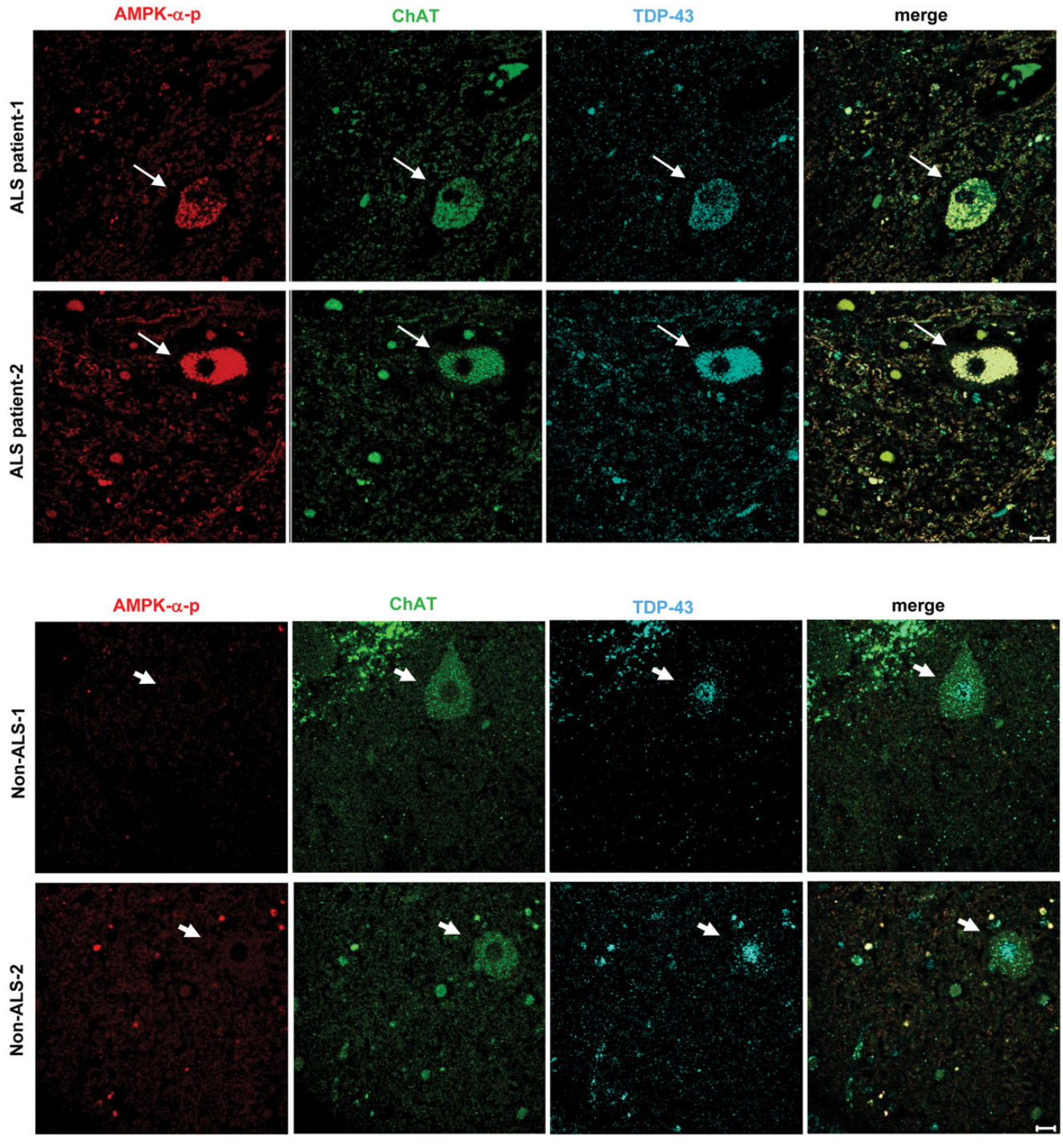

Figure 1. TDP-43 mislocalization is associated with aberrant activation of AMPK in the motor neurons of ALS patients. The spinal cords of ALS patients and age-matched controls were stained for TDP-43 (light blue), phosphorylated AMPK-α at Thr^{172} (AMPK-α-p, red) and the motor neuron marker (ChAT, green). The thick arrows denote normal motor neurons with TDP-43 in the nucleus, while the thin arrows mark motor neurons with the mislocalization of TDP-43 and an enhanced level of AMPK-α-p. Scale bar: 10 μm.

the role of AMPK-α1 in TDP-43 mislocalization, NSC34 cells were transfected with a short hairpin RNA (AMPK-α1-shRNA) for 72 h to down-regulate AMPK-α1 (Fig. 3A and B). As shown in Figure 3C and D, down-regulation of AMPK-α1 greatly reduced the percentage of cells displaying AICAR-induced mislocalization of TDP-43. In addition, expression of a dominant-negative AMPK-α1 mutant (AMPK-α1-T172A-V5) similarly prevented the AICAR-induced TDP-43 mislocalization. In contrast, overexpression of a dominant-positive AMPK-α1 mutant (AMPK-α1-T172D-V5) caused mislocalization of TDP-43 (Fig. 3E and F). In addition, expression of the cytoplasmic form (YFP-AMPK-α1-T172D-NES, (27)), but not the nuclear

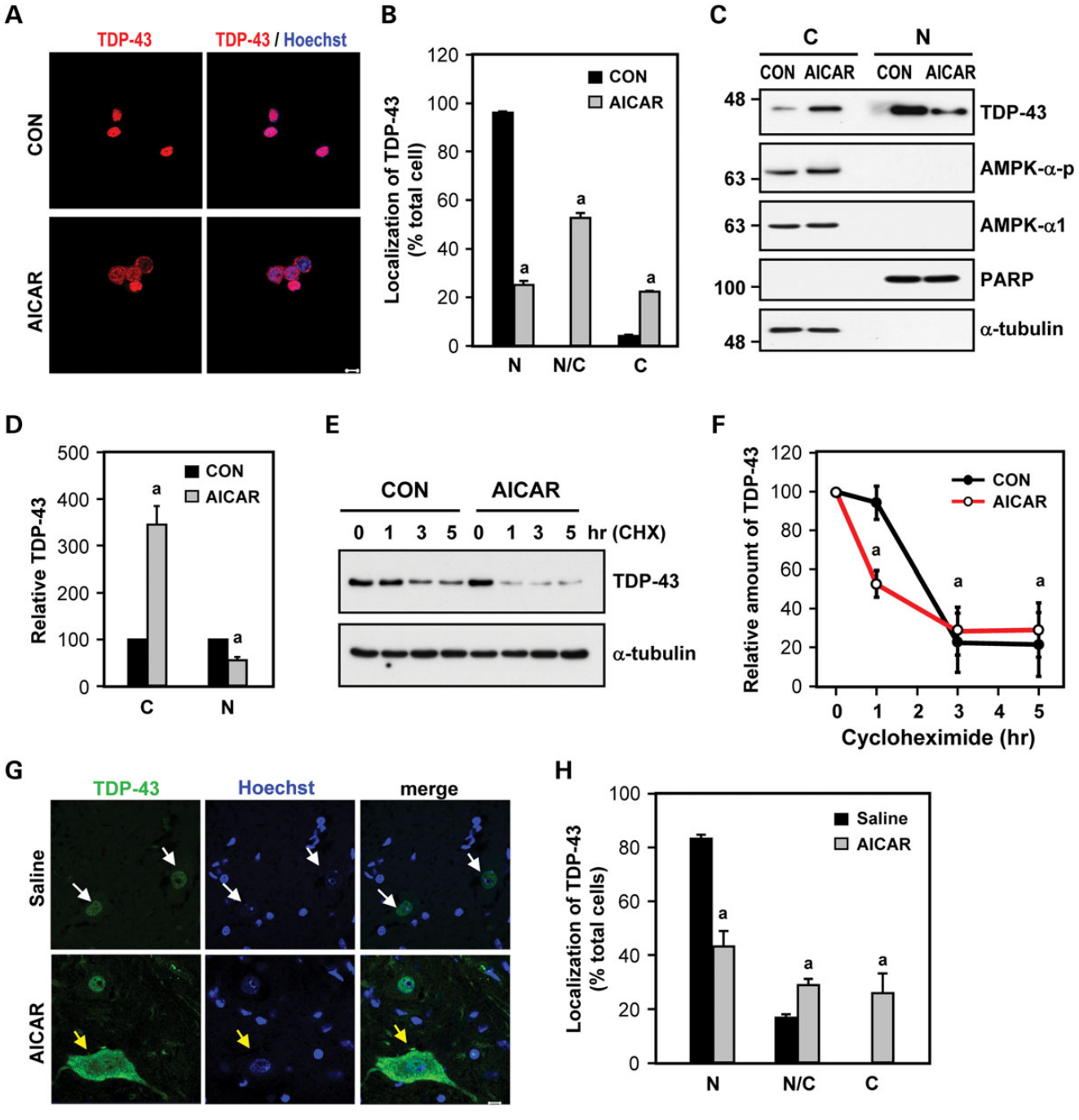

Figure 2. Activation of AMPK led to the mislocalization of TDP-43 in NSC34 cells and in spinal cords of mice. (**A**–**D**) NSC34 cells were treated with an AMPK activator (AICAR, 1 mM) for 24 h. (A and B) The localization of TDP-43 was determined via immunofluorescence staining (TDP-43, red; nuclei, blue). Representative images are presented in (A). As shown in (B), the location of TDP-43 expression was quantified. N, nucleus area; N/C, nucleus and cytoplasm areas; C, cytoplasm area. The data were quantified as the means ± SEM of at least three independent experiments. $^{a}P < 0.05$ versus the control cells. (C and D) The cells were harvested and assessed via western blot analysis. The levels of TDP-43 were normalized to the indicated marker of the nuclear or cytosolic fraction (PARP and α-tubulin, respectively). The data represent the means ± SEM of at least three independent experiments. $^{a}P < 0.05$ versus the control cells. N, nucleus fraction; C, cytoplasmic fraction. (**E** and **F**) The half-life of endogenous TDP-43 in NSC34 cells was examined via a cycloheximide chase assay. The cells were first treated with or without AICAR (1 mM) for 24 h and then with cycloheximide (100 μg/ml) for the indicated periods. The total lysate was harvested, and the expression of TDP-43 was measured by western blot analysis (E). The level of TDP-43 at the indicated time was first normalized to that of α-tubulin and then divided by that of the control group (i.e. before the addition of cycloheximide). (F). The data represent the means ± SEM. $^{a}P < 0.05$ versus the 0 h time point. (**G** and **H**) An AMPK activator (AICAR, 30 μg/5 μl/animal) or saline (control, 5 μl/animal) was injected into the spinal cord of B6 mice ($N = 4$ per group) for 24 h. The cellular localization of TDP-43 was analyzed via immunofluorescence staining (TDP-43, green; nuclei, blue). Representative images are presented in (G). The white arrows denote normal cells with TDP-43 in the nucleus, while the yellow arrows mark cells with the mislocalization of TDP-43. The localization of TDP-43 was quantified and shown in (H). N, nucleus area; N/C, nucleus and cytoplasm areas; C, cytoplasm area. For the quantitation of NSC34 cells, at least 100 cells were counted in each condition. For the mouse spinal cord sections, ∼100 cells were counted. The data represent the means ± SEM. $^{a}P < 0.05$ versus the control. Scale bar: 10 μm.

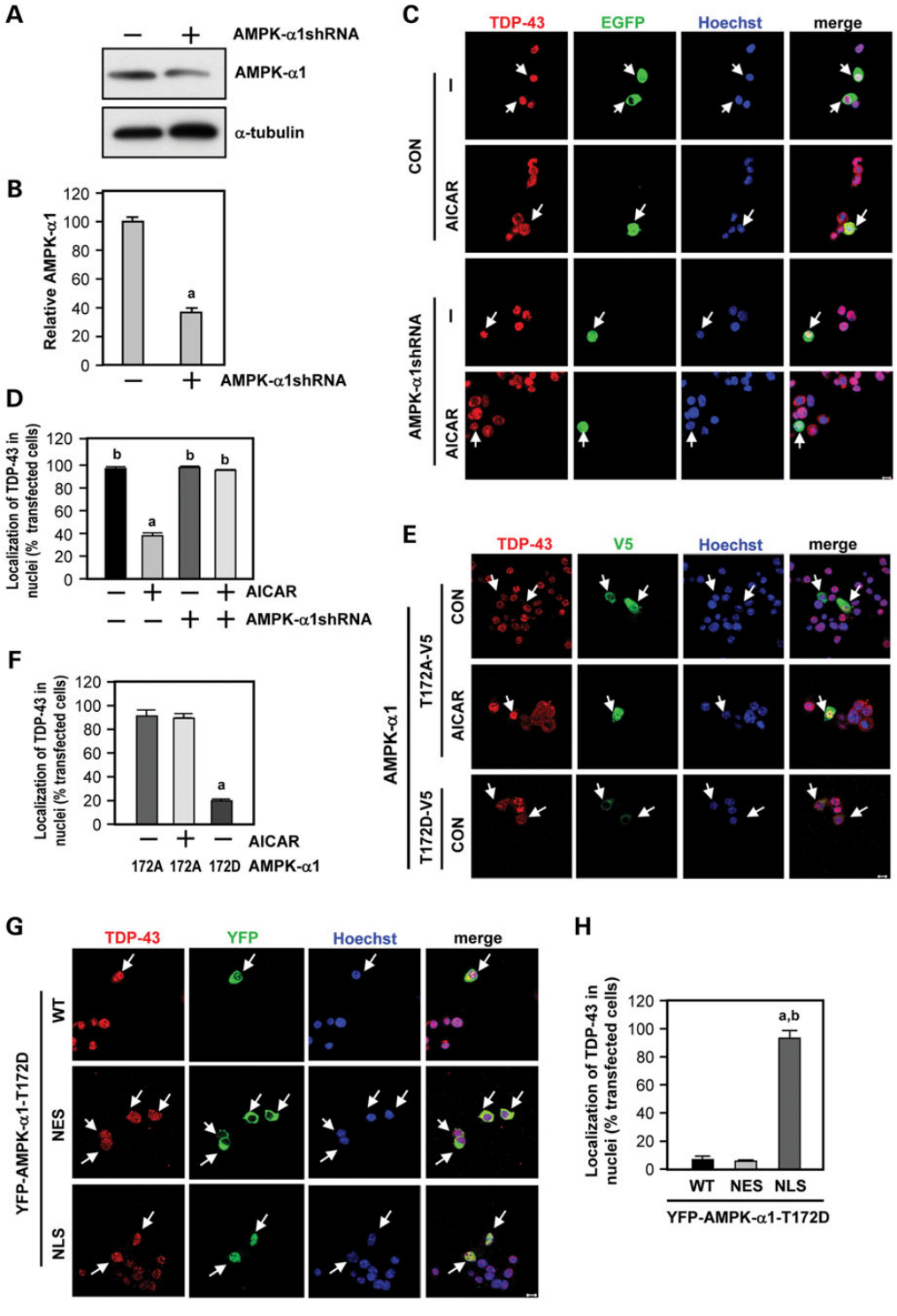

Figure 3. Activation of AMPK-α1 mediates the mislocalization of TDP-43. (**A** and **B**) NSC34 cells were transfected with a short hairpin RNA (AMPK-α1-shRNA) against AMPK-α1 or an empty vector for 72 h. The cells were harvested to analyze the level of AMPK-α1 expression via western blot analysis (A), which was normalized to that of an internal control (α-tubulin). Quantification of the expression level of AMPK-α1 is shown in (B). The data are presented as the means ± SEM. $^{a}P < 0.05$ versus the control cells. (**C** and **D**) NSC34 cells were transfected with the indicated plasmid and a reporter construct (EGFP, green) at a molar ratio of 4 : 1 for 48 h, followed by treatment with AICAR (1 mM) for 24 h. The white arrows denote transfected cells. The localization of TDP-43 was quantified as shown in (D). $^{a}P < 0.05$ versus the control cells. $^{b}P < 0.05$ versus the AICAR-treated cells. (**E**–**H**) NSC34 cells were transfected with the indicated AMPK variant construct for 48 h, followed by treatment with AICAR (1 mM) for 24 h. The localization of TDP-43 was determined via immunofluorescence staining (TDP-43, red; AMPKα1-T172A/D-V5 or YFP-AMPK-α1-T172D, green; nuclei, blue). Representative images are presented in (E) and (G). The localization of TDP-43 was quantified, as shown in (F) and (H). The white arrows indicate transfected cells. The localization of TDP-43 was quantified as the means ± SEM. (F) $^{a}P < 0.05$ versus the cells transfected with AMPK-α1-T172A-V5. (H) $^{a}P < 0.01$ versus the cells transfected with AMPK-α1-T172D-WT-V5; $^{b}P < 0.01$ versus the cells transfected with YFP-AMPK-α1-T172D-NES and treated with AICAR. Scale bar: 10 μm.

form (YFP-AMPK-α1-T172D-NLS, (27)), of the dominant-positive AMPK-α1 mutant triggered TDP-43 mislocalization (Fig. 3G and H). Collectively, our findings demonstrate that aberrant activation of AMPK induces the cytoplasmic mislocalization of TDP-43 in motor neurons. Although activation of AMPK by AICAR was observed readily, the level of TDP-43 phosphorylation at the disease-associated serine residues (i.e. $Ser^{409/410}$ and $Ser^{403/404}$) was not altered (Supplementary Material, Fig. S3). These results suggest that TDP-43 is not a substrate of AMPK.

Mislocalized TDP-43 in the cytoplasm triggers a positive feedback cycle between the activation of AMPK and the elevated production of ROS

A recent report revealed that pathogenic TDP-43 mutant protein, when abnormally expressed in the cytoplasm, co-localized with mitochondria and caused dysfunction (30). Because dysfunctional mitochondria are a major source of ROS, we hypothesized that cytoplasmic mislocalization of TDP-43 may enhance the level of ROS, thus further activating the ROS/AMPK pathway. To evaluate this potential positive feedback cycle between the ROS/AMPK pathway and TDP-43 mislocalization, we expressed WT TDP-43 (EGFP-TDP43) or the cytoplasmic variant (EGFP-TDP43-NLSmt), which contains a mutated nuclear localization signal (NLS), in NSC34 cells. As shown in Figure 4A, the expression of EGFP-TDP43-NLSmt, which was primarily detected in the cytoplasm, elevated the cellular level of ROS based on the signal of a fluorogenic probe (CellROX) that represented cellular oxidative stress. No effect of EGFP or EGFP-TDP43 was detected.

Because AMPK is known to function downstream of ROS to regulate cellular function (31), we next assessed whether the enhancement of ROS in NSC34 cells led to the activation of AMPK. As shown in Figure 4B and C, H_2O_2 treatment enhanced the activation and phosphorylation of AMPK at Thr^{172} (AMPK-α-p). To investigate the effect of oxidative stress on TDP-43 mislocalization (21,32), we treated the NSC34 cells with H_2O_2 (500 μM) for 3 h. Immunocytochemical staining revealed that H_2O_2 treatment shifted TDP-43 from the nucleus to the cytoplasm (Fig. 4D and E). An inhibitor of AMPK (compound C, CC) suppressed the H_2O_2-induced mislocalization of TDP-43 (Fig. 4F and G), suggesting that the oxidative stress-triggered mislocalization of TDP-43 was mediated by AMPK.

Consistent with the above hypothesis, overexpression of EGFP-TDP43-NLSmt that elevated the ROS, but not EGFP or EGFP-TDP-43, increased the activation and phosphorylation of AMPK (Fig. 5A and B). Moreover, treatment with an ROS scavenger (*N*-acetyl-L-cysteine, NAC) reduced AMPK activation (Fig. 5C and D). These results suggest that AMPK activated by ROS causes mislocalization of TDP-43 in NSC34 cells, which in turn elicits cellular oxidative stress and the abnormal activation of AMPK. Thus, the ROS, AMPK and mislocalized TDP-43 result in detriment through a positive feedback mechanism.

Suppression of AMPK using cAMP-stimulating drugs normalizes the mislocalization of TDP-43 and delayed disease progression of ALS

We previously showed that aberrant activation of AMPK activation can be suppressed by activation of the $A_{2A}R$ in striatal neurons in Huntington's disease (27). The $A_{2A}R$ is expressed in the spinal cord and is a drug target for the treatment of spinal cord reperfusion injury (33,34). To evaluate whether activation of the $A_{2A}R$ might provide beneficial effects on ALS, we first treated NSC34 cells with an adenosine analog, which activates the $A_{2A}R$ (35,36). As expected, treatment of NSC34 cells with this $A_{2A}R$ drug (JMF1907) enhanced the activity of adenylyl cyclase (AC) (Fig. 6A) and reduced the AICAR-induced activation/phosphorylation of AMPK (Fig. 6B and C). These effects of JMF1907 were blocked using an $A_{2A}R$-selective antagonist (SCH58261), demonstrating the specific involvement of the $A_{2A}R$. Suppression of AMPK activity by JMF1907 was mediated by PKA because a PKA inhibitor (H89) eliminated the inhibitory effect of JMF1907 on AMPK activation/phosphorylation (Fig. 6B and C). Consistent with our hypothesis that activation of AMPK triggers the mislocalization of TDP-43, JMF1907 prevented the mislocalization of TDP-43 (Fig. 6D and E). The rescuing effect of $A_{2A}R$ drugs on TDP-43 mislocalization was readily prevented by SCH58261 and H89, supporting the importance of the $A_{2A}R$/PKA pathway in the protection against the mislocalization of TDP-43 by suppressing AMPK activation.

Next, to evaluate whether JMF1907 could be used to treat ALS, we used an ALS mouse model (designated TDP-43Tg) (37), which exogenously expressed human TDP-43 driven by the prion promoter. Mice were treated with JMF1907 using ALZET osmotic minipumps (111 mg/mouse/day) from the age of 6 weeks to 23 weeks. Consistent with our previous data, the spinal cord of TDP-43Tg mice that expressed human TDP-43 had a higher level of phosphorylation/activation of AMPK compared with WT mice. Chronic treatment with JMF1907 markedly reduced the activation of AMPK in these mice (Fig. 7A and B). Consistently, this treatment also improved motor function based on rotarod performance (Fig. 7C) and forelimb grip strength (Fig. 7D). Possibly because of genetic drift of the transgenic phenotype (38), the TDP-43Tg mice obtained initially from JAX lived up to the age of 2 years in our animal facility. Therefore, we did not evaluate whether JMF1907 affected the survival of the TDP-43Tg mice. Importantly, no effect of JMF1907 on the body weight of these mice was detected (Fig. 7E), indicating that chronic treatment with JMF1907 did not appear to be toxic in these mice.

It is worth noting that, the amount of total TDP-43 in the spinal cord was not higher in the TDP-43Tg mice used in the present study than in the WT mice, unlike what was reported in the original study (37). This may be explained by the genetic drift of the transgenic phenotype (38). These TDP-43Tg mice, both obtained from the Jackson Laboratories (JAX) and produced in our animal facility, can live longer than 2 years. Nonetheless, the TDP-43Tg mice still expressed human TDP-43 protein in motor neurons. In addition, chronic treatment with JMF1907 markedly reduced the amount of the full-length and the pathogenic low-molecular-weight fragment of human TDP-43 protein in the spinal cord of TDP-43Tg mice. These results support that JMF1907 exerted protective effects on motor neurons and the motor neuron-related phenotypes in TDP-43Tg mice.

Because the expression of human TDP-43 protein in this TDP-43Tg mouse model was also detected in the muscle (37), we performed experiments to show that the level of AMPK phosphorylation and the expression of AMPK-α1 were not altered in the muscle of TDP-43Tg mice and that treatment with JMF1907 had no significant effect (Supplementary Material, Fig. S4A).

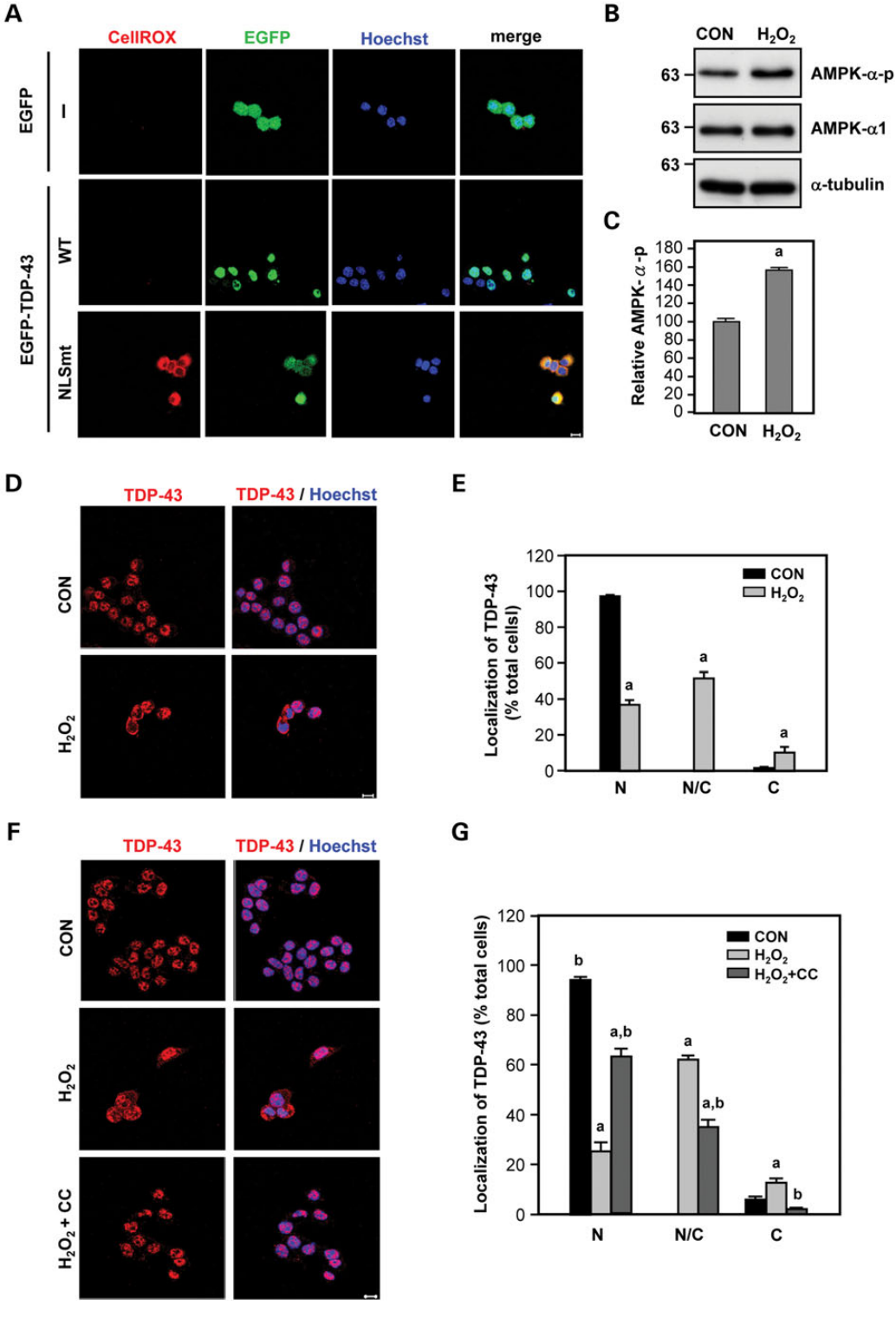

Figure 4. Mislocalized TDP-43 in the cytoplasm results in increased levels of ROS and subsequently triggers TDP-43 mislocalization via AMPK activation. (**A**) NSC34 cells were transfected with the indicated plasmid for 48 h. The level of ROS was analyzed using an ROS detection dye (CellROX) according to the manufacturer's protocol. (**B** and **C**) NSC34 cells were treated with H_2O_2 (500 μM) for 3 h. The activation of AMPK, determined based on the phosphorylation at Thr^{172} (AMPK-α-p), was analyzed via western blot analysis, normalized to the expression level of AMPK-α1. Quantification of the expression level of AMPK-α-p is shown in (C). The data are presented as the means ± SEM. $^{a}P < 0.05$ versus the control cells. (**D** and **E**) NSC34 cells were treated with H_2O_2 (500 μM) for 3 h. (**F** and **G**) The cells were treated with the indicated reagent (H_2O_2, 500 μM and/or CC, 10 μM) for 3 h. (D–G) The localization of TDP-43 was determined via immunofluorescence staining (TDP-43, red, nuclei, blue). Representative images are presented in (D) and (F). The localization of TDP-43 was quantified, as shown in (E) and (G). N, nucleus area; N/C, nucleus and the cytoplasm areas; C, cytoplasm area. At least 100 cells were counted for each condition. The data represent the means ± SEM of at least three independent experiments. $^{a}P < 0.05$ versus the control cells; $^{b}P < 0.05$, H_2O_2 versus H_2O_2 plus CC. Scale bar: 10 μm.

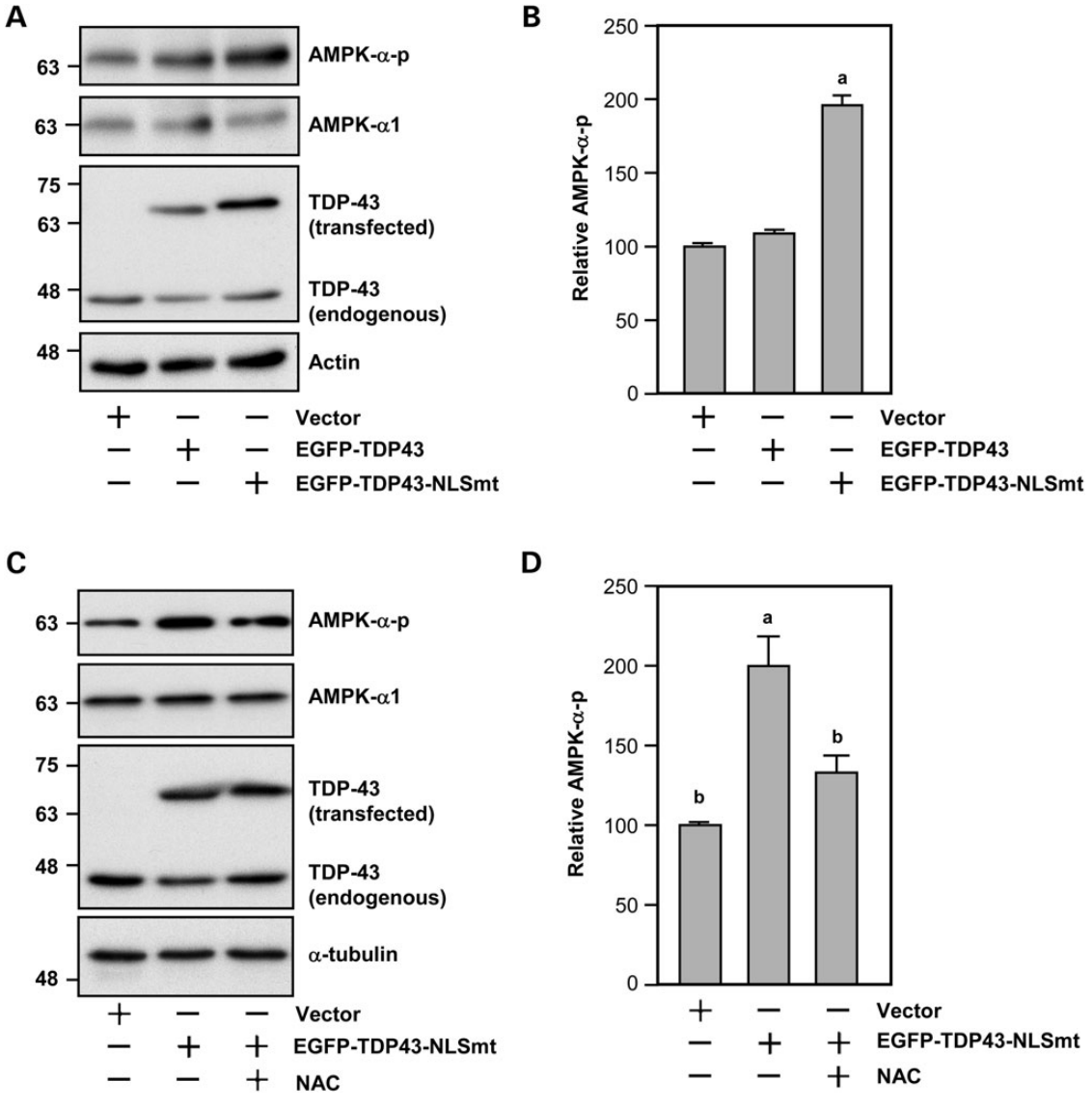

Figure 5. An ROS scavenger (NAC) suppressed the AMPK activation induced by mislocalized TDP-43 in the cytoplasm. (**A** and **B**) NSC34 cells were transfected with the indicated construct for 48 h. The levels of phosphorylated AMPK-α at Thr^{172} (AMPK-α-p) were determined via western blot analysis, normalized to the expression level of AMPK-α1. The data represent the means ± SEM. $^{a}P < 0.05$ versus the cells transfected with the vector. (**C** and **D**) NSC34 cells were transfected with the indicated plasmid in the absence or presence of an anti-oxidant reagent (NAC, 5 mM) for 24 h. The levels of AMPK-α-p were determined via western blot analysis, normalized to the expression level of AMPK-α1. The data represent the means ± SEM. $^{a}P < 0.05$ versus the cells transfected with the vector. $^{b}P < 0.05$ versus the cells transfected with EGFP-TDP43-NLSmt.

Immunohistochemical analyses showed that TDP-43Tg mice exhibited myopathy, presented as an increase in the number of internal nuclei, atrophy and abnormal contour of individual muscle fibers (37), which was not changed by the treatment of JMF1907 (Supplementary Material, Fig. S4B). In addition, JMF1907 did not rescue TDP-43 mislocalization in the muscle of TDP-43Tg mice (Supplementary Material, Fig. S4C). Thus, the beneficial effect of JMF1907 is most likely attributed to the rescue of neurological deficits of spinal cord of TDP-43Tg mice.

DISCUSSION

Cytoplasmic mislocalization of TDP-43 is considered to be an early event important for the pathogenesis of ALS (12); however, the underlying mechanism that modulates the subcellular localization of TDP-43 is largely unknown. Here we demonstrated that dysregulation in the activity of AMPK, a key sensor of metabolic stress, retained TDP-43 in the cytoplasmic compartment. Although the cause of the aberrant activation of AMPK remains to be further studies, we were particularly interested in the role of ROS because oxidative stress, which has been implicated in ALS (14), is known to regulate the nuclear cytoplasmic shuttling of several nuclear transport proteins (e.g. importin-α and CAS) (39). Several lines of evidence in the present study indicate that elevated oxidative stress might cause the abnormal activation of AMPK and subsequent TDP-43 mislocalization (Fig. 4). Our findings are in agreement with earlier studies that ROS is an activator of AMPK

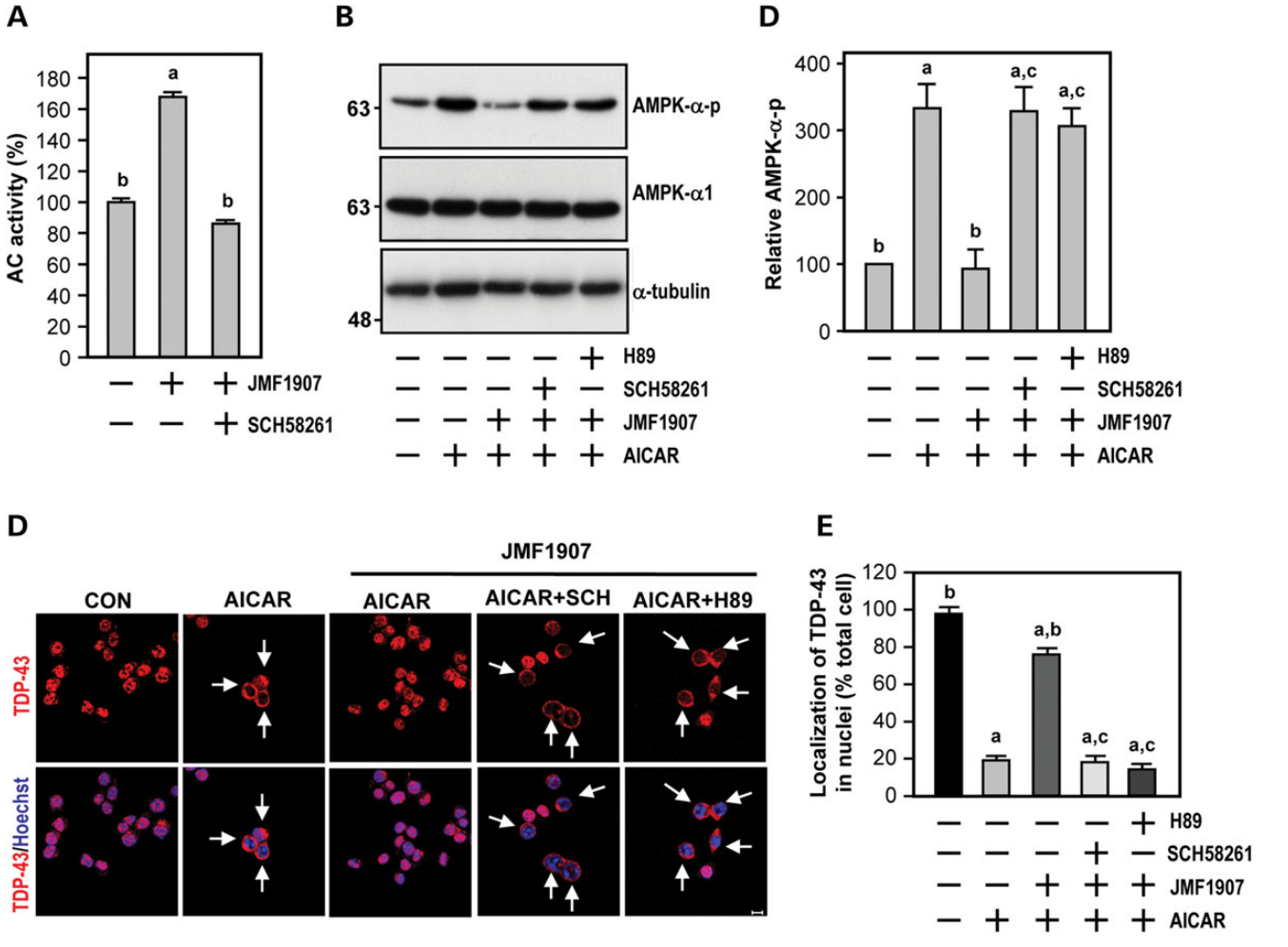

Figure 6. Activation of $A_{2A}R$ using JMF1907 rescued the AMPK-triggered mislocalization of TDP-43. (**A**) NSC34 cells were treated with an $A_{2A}R$ agonist (JMF1907, 30 μM) in the absence or presence of an $A_{2A}R$-selective antagonist (Sch58261, 10 μM) for 20 min at RT. The cells were harvested for the determination of AC activity. $^{a}P < 0.01$ versus the control cells. $^{b}P < 0.01$ versus the JMF1907 treated cells. (**B**–**E**) NSC34 cells were treated with the indicated drug(s) (AICAR, 1 mM; JMF1907 30 μM; Sch58261, 10 μM; and H89, 10 μM) for 24 h. (B and C) The levels of AMPK-α-p was determined via western blot analysis, normalized to the expression level of AMPK-α1. The data represent the means ± SEM. $^{a}P < 0.05$ versus the control cells. $^{b}P < 0.05$ versus the AICAR group. $^{c}P < 0.05$ versus the AICAR plus JMF1907 group. (D and E) The localization of TDP-43 (red) was analyzed via immunofluorescence staining. Representative images are presented in (D). Quantification of the cellular localization of TDP-43 (red) is shown in (E). At least 100 cells were counted for each condition. The data represent the means ± SEM. $^{a}P < 0.05$ versus the control group. $^{b}P < 0.05$ versus the AICAR group. $^{c}P < 0.05$ versus the AICAR plus JMF1907 group. The arrows mark cells with the mislocalization of TDP-43. Scale bar: 10 μm.

(23,24,27). Intriguingly, we found that expression of TDP-43 in the cytoplasmic region alone was sufficient to induce ROS production in NSC34 cells, resulting in the subsequent activation of AMPK (Fig. 5). This cytosolic TDP-43-mediated AMPK activation appeared to be ROS-dependent because an ROS scavenger (NAC) blocked the effect of cytosolic TDP-43 on AMPK activation (Fig. 5D). The ROS/AMPK pathway and the localization of pathogenic TDP-43 to the cytoplasm might regulate one another via a feedforward loop. Consistent with the importance of elevated ROS, cytoplasmic mislocalization of TDP-43 was found in human ALS patients and in mice expressing mutant superoxide dismutase 1 (SOD1), which caused increased production of damaging ROS (32,40–42). In addition, treatment with NAC ameliorated the degeneration of motor neurons and improved motor function in ALS mouse models (43,44). Collectively, the ROS/AMPK pathway and pathogenic TDP-43 mislocalization might be important drug targets for ALS. Therapeutic interventions targeting the ROS/AMPK pathway are likely to delay the progression of ALS.

In the present study, the involvement of AMPK-α1 was supported by the results of down-regulation of AMPK-α1 and expression of dominant-positive AMPK-α1 mutants (AMPK-α1-T172D-V5, YFP-AMPK-α1-NES-T172D; Fig. 3). Intriguingly, upon activation of AMPK, the protein stability of TDP-43 in NSC34 cells was greatly reduced (Fig. 2E and F). This result is consistent with previous studies indicating that the TDP-43 protein displays a relatively short half-life (45). Although the mechanism that mediates the accelerated degradation of TDP-43 by AMPK is currently unknown, this mechanism apparently contributes to the rapid nuclear clearance of TDP-43 upon AMPK activation. As reported previously, the abnormal accumulation of cytosolic TDP-43 is accompanied by nuclear clearance of TDP-43 in ALS patients (2). This abnormal distribution of TDP-43 is believed to

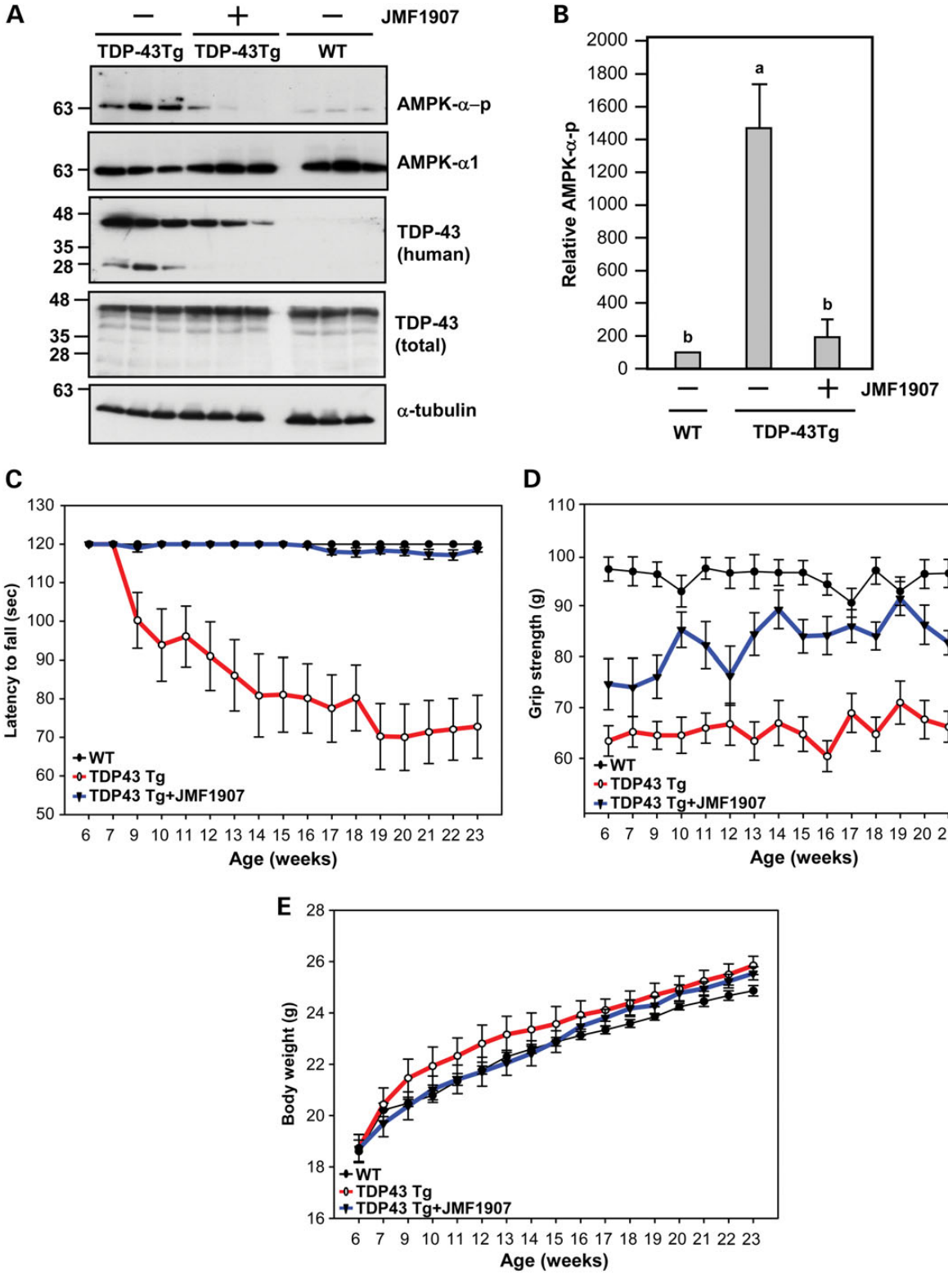

Figure 7. Treatment with JMF1907 improved the motor function of TDP-43 transgenic (TDP-43Tg) mice, an ALS model. JMF1907 (111 mg/mouse/day) or vehicle (CON) was administered subcutaneously to the indicated mice at 6 weeks of age using ALZET osmotic minipumps for 18 weeks, with pumps replaced every 4 weeks. ($n = 15–18$ for each condition). The data represent the means ± SEM. (**A** and **B**) The spinal cords from the indicated mice of 14 weeks were harvested to determine the levels of phosphorylated AMPK-α at Thr^{172} (AMPK-α-p), AMPK-α1 and TDP-43 via western blot analyses (A). The level of phosphorylated AMPK-α at Thr^{172} (AMPK-α-p) was normalized to that of AMPK-α1, as presented in (B). $^{a}P < 0.05$ versus the WT mice. $^{b}P < 0.05$ versus the TDP-43Tg mice. The rotarod performance (**C**) and the grip strength (**D**) were evaluated. $P < 0.05$, TDP-43Tg mice versus WT mice, two-way ANOVA. $P < 0.05$, the TDP-43Tg mice versus the TDP-43Tg mice treated with JMF1907, two-way ANOVA. (**E**) The body weight was determined. No significant difference among all groups tested was found.

cause neuronal atrophy due to the loss of proper functions of TDP-43 in nuclei, as well as toxic gains of function (such as increased ROS levels and AMPK activation, Figs 4 and 5) of TDP-43 in the cytoplasm. Our results suggest that abnormal activation of AMPK plays a key role in regulating the nuclear clearance and cytosolic accumulation of TDP-43. Thus, AMPK is an important drug target for ALS.

Our finding is in agreement with a recent study that found that the activity of AMPK is elevated in the spinal cord of mSOD1 mice (25). In that study, the authors highlighted the importance of AMPK-α2 because down-regulation of the AMPK-α2 ortholog in *C. elegans* produced a beneficial effect. The downstream target of AMPK-α2 was not investigated (25). Our study clearly demonstrated that AMPK-α1 also plays a critical role in ALS. One possible downstream target of AMPK-α1 is importin-α1 because it is a substrate of AMPK-α1 and it mediates the nuclear import of TDP-43 (46,47). The role of importin-α1 in the AMPK-mediated ALS pathogenesis is of great interest and needs further investigation. During the preparation of this manuscript, Kim and colleagues revealed that the level of phosphorylated eIF2α, a eukaryotic initiation factor and a substrate of AMPK (48), is increased during TDP-43 proteinopathy and plays a detrimental role (49). The involvement of other AMPK substrates in the development of ALS requires attention and further investigation.

During the preparation of this manuscript, Perera and colleagues reported an interesting observation that AMPK is activated in the spinal cord of $SOD1^{G93A}$ mice but is markedly suppressed in the spinal cord of transgenic $TDP\text{-}43^{A315T}$ mice (50). These authors suggested that TDP-43 mutants causes inhibition of AMPK by increased expression of protein phosphatase 2A, which dephosphorylates and thus inactivates AMPK. In that study, TDP-43 mutants (including $TDP\text{-}43^{A315T}$) exhibited a stronger ability to inactivate AMPK than did WT TDP-43 in NSC34 cells. No effect of WT TDP-43 was evaluated in NSC34 cells or *in vivo*. In the present study, we found that expression of WT TDP-43 caused the activation of AMPK in the spinal cord of TDP-43Tg mice. The findings of Perera and colleagues are consistent with our hypothesis that AMPK is abnormally regulated in ALS mouse models and that the in-depth investigation of the role of AMPK in ALS is a timely issue. For example, further evaluation and comparison of the temporal regulation of AMPK during disease progression in mice exogenously expressing WT or mutant TDP-43 proteins would provide important insights into TDP proteinopathy and ALS pathogenesis in motor neurons.

AMPK is a central energy sensor that can be upregulated by multiple signaling pathways triggered by environmental insults (24). With respect to ALS patients, premorbid fitness and increased resting energy expenditure have been reported (6,51). Because activators of AMPK have been used to treat metabolic diseases, including type II diabetes (52), the potential involvement of AMPK in ALS is thus a timely issue. For example, Kaneb and colleagues demonstrated that metformin, an activator of AMPK and a first-line drug for type II diabetes (53), exerted harmful effects on female ALS mice and might be detrimental to female ALS patients suffering from type II diabetes. Therefore, further investigations on the potential effect of aberrant AMPK activation on the degeneration of motor neurons in both familial and sporadic ALS are critical.

In summary, the results of the present study demonstrate that cellular stress (including elevated ROS levels and accumulation of TDP-43 in the cytoplasm) caused aberrant activation of AMPK and initiated a critical pathogenic pathway in motor neurons in ALS (Fig. 8). Stimulation of $A_{2A}R$ using small molecules normalized the abnormal activation of AMPK and produced beneficial effects on the progression of ALS in a mouse model of ALS (Figs 6 and 7). Our finding also suggests that $A_{2A}R$ and PKA are novel drug targets for ALS. Consistently, a recent study reported that chronic treatment with caffeine, a non-specific antagonist of $A_{2A}R$, is detrimental in an ALS mouse model (SOD1-G93A) (54). Therefore, further evaluation of drugs that stimulate $A_{2A}R$ or enhance the cAMP level are of warranted.

MATERIALS AND METHODS

Cell culture

The NSC34 motoneuron-like cell line, a kind gift from Dr Cashman (55), was maintained in Dulbecco's modified Eagle's medium containing 10% fetal bovine serum and 1% penicillin–streptomycin (Invitrogen GibcoBRL, Carlsbad, CA, USA) in 5% CO_2 at 37°C. The cells were transfected with the indicated plasmid using Lipofectamine 2000 (Invitrogen GibcoBRL) for 48–72 h.

Constructs

DNA fragments containing TDP-43 variants were generated by standard PCR reactions of human TDP-43 and were cloned into

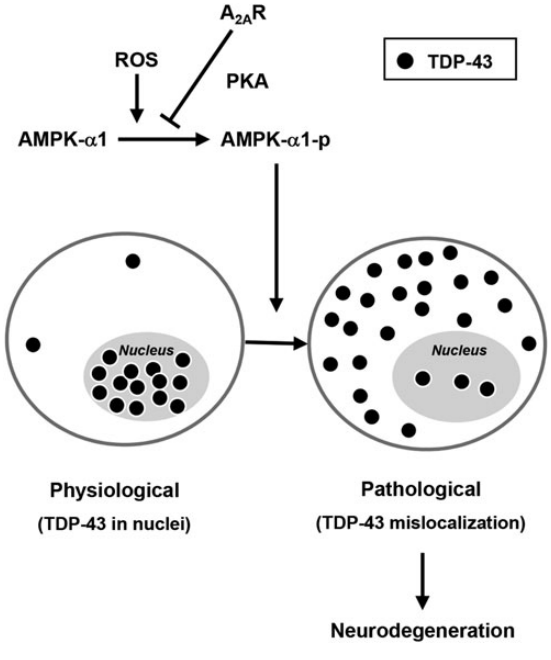

Figure 8. Schematic representation of the signaling pathway by which $A_{2A}R$ activity rescues the detrimental effect of AMPK-α1 on TDP-43 mislocalization. Under physiological conditions, TDP-43 (closed circles) is primarily expressed in the nucleus. Upon oxidative stress, AMPK-α1 becomes activated, triggers mislocalization of TDP-43 and leads to detrimental effects and ultimately causes atrophy of motor neurons. Stimulation of $A_{2A}R$ activates the cAMP-dependent PKA pathway, which inhibits AMPK and rescues the mislocalization of TDP-43.

the pEGFP-C3 vector (Clontech Laboratories, Mountain View, CA, USA). The resultant fragments of TDP-43 variants were verified by DNA sequencing. All AMPK variants were constructed and subcloned into pcDNA3 (Invitrogen Life Technologies, Carlsbad, CA, USA) as described elsewhere (27). The sequence (5′-CCCATCAGCAACTATCGATCTTTTCAAGA GAAAGATCGATA-GTTGCTGATTTTTTGGAAA-3′) of a short hairpin RNA (AMPK-α1-shRNA) against AMPK-α1 was subcloned into the pSUPER vector and characterized earlier (27).

Animals and drug administration

The ALS mice (B6SJL-Tg(Prnp-TARDBP)4Jlel/J;(37)) were purchased from the Jackson Laboratory (Bar Harbor, ME, USA) and bred by the National Laboratory Animal Center in Tainan. The offspring was genotyped via PCR using the forward primer 5′-GGTGGTGGGATGAACTTTGG-3′ and the reverse primer 5′-GTGGATAACCCCTCCCCC AGCCTA GAC-3′. Littermate WT controls were used in all experiments. JMF1907 (111 mg/mouse/day) or vehicle (saline) was administered subcutaneously to each mouse at 6 weeks of age using a 4 week ALZET osmotic minipump (ALZET, Cupertino, CA, USA) for 18 weeks; the pumps were replaced every 4 weeks as indicated in the manufacturer's protocol. The animal experiments were performed under protocols that were approved by the Academia Sinica Institutional Animal Care and Utilization Committee in Taiwan.

Intrathecal injection

Male 2- to 3-month-old C57BL/6 mice were anesthetized by intraperitoneal injection (i.p.) of ketamine (100 mg/kg) plus xylazine (7.5 mg/kg). A 1–1.5 cm incision was made in the epidermis of the anesthetized mouse for intrathecal injection into the space between L4 and L6, the region most suitable for intrathecal injection (56). The indicated drug or saline (5 μl) was injected using a 10-μl Hamilton syringe with 30-gauge 1/2-in. needle. Twenty-four hours after the injection, the mouse was sacrificed, and the spinal cord tissues between L4 and L6 were collected.

Sample preparation, western blot and SDS–PAGE

Spinal cord and muscle samples were placed carefully on ice, chopped into small pieces and homogenized in ice-cold radioimmunoprecipitation assay buffer (50 mM Tris–HCl, 0.5% sodium deoxycholate, 1% Triton X-100 and 150 mM NaCl) containing 1 mM PMSF, 1 mM Na_3VO_4, 0.5 mg/ml aprotinin, 0.1 mM leupeptin and 4 mM pepstatin for further biochemical analyses.

NSC34 cells were fractionated using a protein extraction kit (Fermentas, Thermo Fisher Scientific, Waltham, MA, USA). Briefly, cells were centrifuged at 250*g* for 5 min and washed extensively with ice-cold PBS. The cytoplasmic and nuclear fractions were prepared sequentially using the corresponding buffer and following the manufacturer's protocol.

Western blot analyses were performed as described previously (27). Briefly, the samples were separated via electrophoresis using 10% SDS–polyacrylamide gels and were electrotransferred to polyvinylidene difluoride membranes (Millipore, Billerica, MA, USA). The following primary antibodies were used for the indicated experiments: anti-AMPK-α-pT172 (1:1000; Cell Signaling Technology; Danvers, MA, USA), anti-AMPK-α1 (1:1000; GeneTex; Irvine, CA, USA or Novus; Biologicals Littleton, CO, USA), anti-TDP-43 (1:1000; Abcam; Cambridge, MA, USA), anti-TDP-43 (1:1000; Abnova; Taipei, Taiwan), self-generated TDP-43 polyclonal antiserum was provided by Dr Pang-Hsien Tu laboratory to against the mouse and human TDP-43 (1:5000; LTK Biolaboratories, Taiwan) (57), anti-poly(ADP-ribose) polymerase (PARP; 1:2000; Millipore) and anti-α-tubulin (1:10 000; Sigma-Aldrich; St. Louis, MO, USA). The immunoreactive signals were detected using ECL reagents (PerkinElmer; Waltham, MA, USA).

Immunocytochemical staining and histochemistry

The cells were fixed using −20°C methanol for 10 min, washed with PBS at room temperature (RT) three times for 5 min each, and blocked using 2% normal goat serum and 2% bovine serum albumin (BSA) in PBS for 1 h at RT. The cells were then incubated in the desired primary antibody at 4°C for 18–22 h, followed by incubation in the corresponding secondary antibody for 1 h at RT. The fluorescently immunostained samples were analyzed using a confocal microscope (LSM 510, Carl Zeiss; Oberkochen, Germany) and MetaMorph software (Universal Imaging Corporation, Chester, PA, USA).

To prepare spinal cord tissues for immunocytochemical staining, mice were anesthetized by i.p. injection of pentobarbital (100 mg/ml) and perfused with 4% paraformaldehyde. The spinal cord tissues between L4 and L6 were removed carefully, postfixed with 4% paraformaldehyde overnight and stored in 0.1 M phosphate buffer containing 30% sucrose over two nights at 4°C, embedded in OCT medium and sectioned into 18-μm-thick sections on a cryomicrotome at −20°C. Immunohistochemical staining of the mouse spinal cord sections was performed as described previously (27). Briefly, the sections were blocked with 3% BSA and then incubated with the indicated primary antibody (anti-TDP-43, 1:500, Abcam) for 36–40 h in PBS containing 1% BSA at 4°C. The sections were washed extensively and incubated with the corresponding secondary antibody for 2 h at RT. The nuclei were stained with Hoechst 33258. The samples were analyzed using a confocal microscope (LSM780; Carl Zeiss). Three frames from five sections spaced evenly between L4 and L6 were assessed for each mouse. At least 10 neurons were scored for each animal.

For hematoxylin and eosin (H&E) staining of the muscle, hindlimb skeletal muscles were fixed in cold isopropanol and stored in liquid nitrogen. The cryostat sections (5 μm) were prepared on a cryomicrotome at −20°C. H&E staining was performed as described previously (37).

Human spinal cord sections

The spinal cord and brain sections were obtained from the NICHD Brain and Tissue Bank for Developmental Disorders (University of Maryland, Baltimore, MD, USA). The demographic data and the neuropathology of the spinal cords of these patients are summarized in Table 1. Immunohistochemical staining of the human spinal cord sections (5 μm) was performed as previously described (27). In brief, the sections were

incubated with the indicated primary antibody (anti-human TDP-43, 1:500, Abnova; anti-ChAT, 1:100, Millipore) for 24 h in PBS containing 1% BSA at 4°C. Then, the sections were washed extensively and incubated in an anti-AMPK-α-p antibody for another 48 h, followed by a 2 h-incubation in the corresponding secondary antibodies at RT. The nuclei were stained using Hoechst 33258. The samples were analyzed using a confocal microscope (LSM 510, Zeiss)

Grip strength

The grip strength was measured using a Grip Strength-Meter (TSE Systems, Inc., MO, USA). Briefly, a mouse was grabbed by its tail using a hand and allowed to grasp the height-adjustable grip mounted on a force sensor. A pulling force was applied to the mouse by its tail. The maximum force was indicated on the digital display panel of a connected control unit when the mouse released its grip. Each mouse was examined using three repeated trials.

Rotarod performance

The rotarod assay was performed using a Rotarod apparatus (UGO BASILE, Comerio, Italy) to detect the motor activity of mice at a constant speed of 40 rpm for up to 2 min. The animals were subjected to this assay three times per week, and the latency to fall was recorded.

ROS detection

The cells were incubated in CellROX® (5 μM; Life Technologies Corporation, Carlsbad, CA, USA) for 30 min at 37°C, washed extensively using PBS, and then fixed using 4% paraformaldehyde in PBS at RT for 30 min, followed by immunocytochemical staining, performed as described above.

Protein stability analysis

The cells were treated with cycloheximide (100 μg/mL; Sigma) at different time points. Then, the cells were lysed and the level of TDP-43 expression was detected via western blot analysis. The relative expression level of TDP-43 was quantified as the mean ± SEM.

Adenylyl cyclase activity

The AC assay of the plasma membrane fraction was performed as described previously (58). Briefly, the AC activity was carried out in an AC assay buffer (6 mM $MgCl_2$, 0.2 mM EGTA, 100 mM NaCl, 50 mM HEPES, 1 mM ATP, 1 μM GTP and 0.5 mM 3-isobutyl-1-methylxanthine) for 10 min at 37°C. To stop the reaction, trichloroacetic acid (final concentration = 6%) was added to the reaction mixture. The amount of cAMP was measured by using a radioimmunoassay method as described elsewhere (58).

Statistics

The data were quantified as the means ± SEM of triplicate samples. Each experiment was repeated at least three times. Comparisons between multiple groups were performed using one-way analysis of variance (ANOVA) followed by the *post hoc* Student–Newman–Keuls test. A P-value of <0.05 was considered to be significant.

SUPPLEMENTARY MATERIAL

Supplementary Material is available at *HMG* online.

ACKNOWLEDGEMENTS

We are grateful to Mr Chein-Hung Ho for technical support.

Conflict of Interest statement. One patent application regarding the possible therapeutic use of JMF1907 in patients with neurodegenerative diseases were submitted to patent offices in the US, China, India, Korea, and Taiwan. This patent application was recently approved in Taiwan, but remains to be pending in the other four countries.

FUNDING

This work was supported by grants from the National Science Council (NSC 100-2325-B001-003, NSC 101-2325-B-001-003, NSC 102-2325-B-001-003 and NSC 102-2321-B-001-068-MY3) and the Institute of Biomedical Sciences of Academia Sinica.

REFERENCES

1. Bento-Abreu, A., Van Damme, P., Van Den Bosch, L. and Robberecht, W. (2010) The neurobiology of amyotrophic lateral sclerosis. *Eur. J. Neurosci.*, **31**, 2247–2265.
2. Neumann, M., Sampathu, D.M., Kwong, L.K., Truax, A.C., Micsenyi, M.C., Chou, T.T., Bruce, J., Schuck, T., Grossman, M., Clark, C.M. *et al.* (2006) Ubiquitinated TDP-43 in frontotemporal lobar degeneration and amyotrophic lateral sclerosis. *Science*, **314**, 130–133.
3. Talbot, K. (2011) Familial versus sporadic amyotrophic lateral sclerosis – a false dichotomy? *Brain*, **134**, 3429–3431.
4. Byrne, S., Walsh, C., Lynch, C., Bede, P., Elamin, M., Kenna, K., McLaughlin, R. and Hardiman, O. (2011) Rate of familial amyotrophic lateral sclerosis: a systematic review and meta-analysis. *J. Neurol. Neurosurg. Psychiatry*, **82**, 623–627.
5. Talbot, K. (2009) Another gene for ALS: mutations in sporadic cases and the rare variant hypothesis. *Neurology*, **73**, 1172–1173.
6. Al-Chalabi, A. and Hardiman, O. (2013) The epidemiology of ALS: a conspiracy of genes, environment and time. *Nat. Rev. Neurol.*, **9**, 617–628.
7. Siciliano, G., Carlesi, C., Pasquali, L., Piazza, S., Pietracupa, S., Fornai, F., Ruggieri, S. and Murri, L. (2010) Clinical trials for neuroprotection in ALS. *CNS Neurol. Disord. Drug Targets*, **9**, 305–313.
8. Wang, I.F., Wu, L.S., Chang, H.Y. and Shen, C.K. (2008) TDP-43, the signature protein of FTLD-U, is a neuronal activity-responsive factor. *J. Neurochem.*, **105**, 797–806.
9. Buratti, E., De Conti, L., Stuani, C., Romano, M., Baralle, M. and Baralle, F. (2010) Nuclear factor TDP-43 can affect selected microRNA levels. *FEBS J.*, **277**, 2268–2281.
10. Buratti, E., De Conti, L., Stuani, C., Romano, M., Baralle, M. and Baralle, F. (2010) Nuclear factor TDP-43 can affect selected microRNA levels. *FEBS J.*, **277**, 2268–2281.
11. Giordana, M.T., Piccinini, M., Grifoni, S., De Marco, G., Vercellino, M., Magistrello, M., Pellerino, A., Buccinna, B., Lupino, E. and Rinaudo, M.T. (2009) TDP-43 redistribution is an early event in sporadic amyotrophic lateral sclerosis. *Brain Pathol.*, **20**, 351–360.

12. Lagier-Tourenne, C., Polymenidou, M. and Cleveland, D.W. (2010) TDP-43 and FUS/TLS: emerging roles in RNA processing and neurodegeneration. *Hum. Mol. Genet.*, **19**, R46–R64.
13. Urushitani, M., Sato, T., Bamba, H., Hisa, Y. and Tooyama, I. (2010) Synergistic effect between proteasome and autophagosome in the clearance of polyubiquitinated TDP-43. *J. Neurosci. Res.*, **88**, 784–797.
14. D'Amico, E., Factor-Litvak, P., Santella, R.M. and Mitsumoto, H. (2013) Clinical perspective on oxidative stress in sporadic amyotrophic lateral sclerosis. *Free Radic. Biol. Med.*, **65**, 509–527.
15. Cohen, T.J., Hwang, A.W., Unger, T., Trojanowski, J.Q. and Lee, V.M. (2012) Redox signalling directly regulates TDP-43 via cysteine oxidation and disulphide cross-linking. *EMBO J.*, **31**, 1241–1252.
16. Capitanio, D., Vasso, M., Ratti, A., Grignaschi, G., Volta, M., Moriggi, M., Daleno, C., Bendotti, C., Silani, V. and Gelfi, C. (2012) Molecular signatures of amyotrophic lateral sclerosis disease progression in hind and forelimb muscles of an SOD1(G93A) mouse model. *Antioxid. Redox Signal.*, **17**, 1333–1350.
17. Wang, P. and Jin, T. (2010) Hydrogen peroxide stimulates nuclear import of the POU homeodomain protein Oct-1 and its repressive effect on the expression of Cdx-2. *BMC Cell Biol.*, **11**, 56.
18. Wang, W., Fan, J., Yang, X., Furer-Galban, S., Lopez de Silanes, I., von Kobbe, C., Guo, J., Georas, S.N., Foufelle, F., Hardie, D.G. *et al.* (2002) AMP-activated kinase regulates cytoplasmic HuR. *Mol. Cell Biol.*, **22**, 3425–3436.
19. Kodiha, M., Crampton, N., Shrivastava, S., Umar, R. and Stochaj, U. (2010) Traffic control at the nuclear pore. *Nucleus*, **1**, 237–244.
20. Kosako, H., Yamaguchi, N., Aranami, C., Ushiyama, M., Kose, S., Imamoto, N., Taniguchi, H., Nishida, E. and Hattori, S. (2009) Phosphoproteomics reveals new ERK MAP kinase targets and links ERK to nucleoporin-mediated nuclear transport. *Nat. Struct. Mol. Biol.*, **16**, 1026–1035.
21. Ayala, V., Granado-Serrano, A.B., Cacabelos, D., Naudi, A., Ilieva, E.V., Boada, J., Caballo-Miralles, V., Llado, J., Ferrer, I., Pamplona, R. *et al.* (2011) Cell stress induces TDP-43 pathological changes associated with ERK1/2 dysfunction: implications in ALS. *Acta Neuropathol.*, **122**, 259–270.
22. Long, Y.C. and Zierath, J.R. (2006) AMP-activated protein kinase signaling in metabolic regulation. *J. Clin. Invest.*, **116**, 1776–1783.
23. Hardie, D.G., Ross, F.A. and Hawley, S.A. (2012) AMPK: a nutrient and energy sensor that maintains energy homeostasis. *Nat. Rev. Mol. Cell Biol.*, **13**, 251–262.
24. Ju, T.C., Lin, Y.S. and Chern, Y. (2012) Energy dysfunction in Huntington's disease: insights from PGC-1alpha, AMPK, and CKB. *Cell Mol. Life Sci.*, **69**, 4107–4120.
25. Lim, M.A., Selak, M.A., Xiang, Z., Krainc, D., Neve, R.L., Kraemer, B.C., Watts, J.L. and Kalb, R.G. (2012) Reduced activity of AMP-activated protein kinase protects against genetic models of motor neuron disease. *J. Neurosci.*, **32**, 1123–1141.
26. Vingtdeux, V., Davies, P., Dickson, D.W. and Marambaud, P. (2011) AMPK is abnormally activated in tangle- and pre-tangle-bearing neurons in Alzheimer's disease and other tauopathies. *Acta Neuropathol.*, **121**, 337–349.
27. Ju, T.C., Chen, H.M., Lin, J.T., Chang, C.P., Chang, W.C., Kang, J.J., Sun, C.P., Tao, M.H., Tu, P.H., Chang, C. *et al.* (2011) Nuclear translocation of AMPK-alpha1 potentiates striatal neurodegeneration in Huntington's disease. *J. Cell Biol.*, **194**, 209–227.
28. Hawley, S.A., Davison, M., Woods, A., Davies, S.P., Beri, R.K., Carling, D. and Hardie, D.G. (1996) Characterization of the AMP-activated protein kinase kinase from rat liver and identification of threonine 172 as the major site at which it phosphorylates AMP-activated protein kinase. *J. Biol. Chem.*, **271**, 27879–27887.
29. Corton, J.M., Gillespie, J.G., Hawley, S.A. and Hardie, D.G. (1995) 5-aminoimidazole-4-carboxamide ribonucleoside. A specific method for activating AMP-activated protein kinase in intact cells? *Eur. J. Biochem.*, **229**, 558–565.
30. Wang, W., Li, L., Lin, W.L., Dickson, D.W., Petrucelli, L., Zhang, T. and Wang, X. (2013) The ALS disease-associated mutant TDP-43 impairs mitochondrial dynamics and function in motor neurons. *Hum. Mol. Genet.*, **22**, 4706–4719.
31. Chen, L., Xu, B., Liu, L., Luo, Y., Yin, J., Zhou, H., Chen, W., Shen, T., Han, X. and Huang, S. (2010) Hydrogen peroxide inhibits mTOR signaling by activation of AMPKalpha leading to apoptosis of neuronal cells. *Lab. Invest.*, **90**, 762–773.
32. Shan, X., Vocadlo, D. and Krieger, C. (2009) Mislocalization of TDP-43 in the G93A mutant SOD1 transgenic mouse model of ALS. *Neurosci. Lett.*, **458**, 70–74.
33. Cassada, D.C., Tribble, C.G., Kaza, A.K., Fiser, S.M., Long, S.M., Linden, J., Rieger, J.M., Kron, I.L. and Kern, J.A. (2001) Adenosine analogue reduces spinal cord reperfusion injury in a time-dependent fashion. *Surgery*, **130**, 230–235.
34. Kaelin-Lang, A., Lauterburg, T. and Burgunder, J.M. (1999) Expression of adenosine A2a receptors gene in the olfactory bulb and spinal cord of rat and mouse. *Neurosci. Lett.*, **261**, 189–191.
35. Chen, J.B., Liu, E.M., Chern, T.R., Yang, C.W., Lin, C.I., Huang, N.K., Lin, Y.L., Chern, Y., Lin, J.H. and Fang, J.M. (2011) Design and synthesis of novel dual-action compounds targeting the adenosine A(2A) receptor and adenosine transporter for neuroprotection. *Chem. Med. Chem.*, **6**, 1390–1400.
36. Huang, N.K., Lin, J.H., Lin, J.T., Lin, C.I., Liu, E.M., Lin, C.J., Chen, W.P., Shen, Y.C., Chen, H.M., Chen, J.B. *et al.* (2011) A new drug design targeting the adenosinergic system for Huntington's disease. *PLoS ONE*, **6**, e20934.
37. Stallings, N.R., Puttaparthi, K., Luther, C.M., Burns, D.K. and Elliott, J.L. (2010) Progressive motor weakness in transgenic mice expressing human TDP-43. *Neurobiol. Dis.*, **40**, 404–414.
38. Davis, J., Maillet, M., Miano, J.M. and Molkentin, J.D. (2012) Lost in transgenesis: a user's guide for genetically manipulating the mouse in cardiac research. *Circ. Res.*, **111**, 761–777.
39. Kodiha, M., Tran, D., Morogan, A., Qian, C. and Stochaj, U. (2009) Dissecting the signaling events that impact classical nuclear import and target nuclear transport factors. *PLoS ONE*, **4**, e8420.
40. Robertson, J., Sanelli, T., Xiao, S., Yang, W., Horne, P., Hammond, R., Pioro, E.P. and Strong, M.J. (2007) Lack of TDP-43 abnormalities in mutant SOD1 transgenic mice shows disparity with ALS. *Neurosci. Lett.*, **420**, 128–132.
41. Boillee, S. and Cleveland, D.W. (2008) Revisiting oxidative damage in ALS: microglia, Nox, and mutant SOD1. *J. Clin. Invest.*, **118**, 474–478.
42. Pokrishevsky, E., Grad, L.I., Yousefi, M., Wang, J., Mackenzie, I.R. and Cashman, N.R. (2012) Aberrant localization of FUS and TDP43 is associated with misfolding of SOD1 in amyotrophic lateral sclerosis. *PLoS ONE*, **7**, e35050.
43. Henderson, J.T., Javaheri, M., Kopko, S. and Roder, J.C. (1996) Reduction of lower motor neuron degeneration in wobbler mice by N-acetyl-L-cysteine. *J. Neurosci.*, **16**, 7574–7582.
44. Andreassen, O.A., Dedeoglu, A., Klivenyi, P., Beal, M.F. and Bush, A.I. (2000) N-acetyl-L-cysteine improves survival and preserves motor performance in an animal model of familial amyotrophic lateral sclerosis. *Neuroreport*, **11**, 2491–2493.
45. Wu, L.S., Cheng, W.C. and Shen, C.K. (2013) Similar dose-dependence of motor neuron cell death caused by wild type human TDP-43 and mutants with ALS-associated amino acid substitutions. *J. Biomed. Sci.*, **20**, 33.
46. Nishimura, A.L., Zupunski, V., Troakes, C., Kathe, C., Fratta, P., Howell, M., Gallo, J.M., Hortobagyi, T., Shaw, C.E. and Rogelj, B. (2010) Nuclear import impairment causes cytoplasmic trans-activation response DNA-binding protein accumulation and is associated with frontotemporal lobar degeneration. *Brain*, **133**, 1763–1771.
47. Wang, W., Yang, X., Kawai, T., Lopez de Silanes, I., Mazan-Mamczarz, K., Chen, P., Chook, Y.M., Quensel, C., Kohler, M. and Gorospe, M. (2004) AMP-activated protein kinase-regulated phosphorylation and acetylation of importin alpha1: involvement in the nuclear import of RNA-binding protein HuR. *J. Biol. Chem.*, **279**, 48376–48388.
48. Dagon, Y., Avraham, Y. and Berry, E.M. (2006) AMPK activation regulates apoptosis, adipogenesis, and lipolysis by eIF2alpha in adipocytes. *Biochem. Biophys. Res. Commun.*, **340**, 43–47.
49. Kim, H.J., Raphael, A.R., Ladow, E.S., McGurk, L., Weber, R.A., Trojanowski, J.Q., Lee, V.M., Finkbeiner, S., Gitler, A.D. and Bonini, N.M. (2014) Therapeutic modulation of eIF2alpha phosphorylation rescues TDP-43 toxicity in amyotrophic lateral sclerosis disease models. *Nat. Genet.*, **46**, 152–160.
50. Perera, N.D., Sheean, R.K., Scott, J.W., Kemp, B.E., Horne, M.K. and Turner, B.J. (2014) Mutant TDP-43 deregulates AMPK activation by PP2A in ALS models. *PLoS ONE*, **9**, e90449.
51. Vaisman, N., Lusaus, M., Nefussy, B., Niv, E., Comaneshter, D., Hallack, R. and Drory, V.E. (2009) Do patients with amyotrophic lateral sclerosis (ALS) have increased energy needs? *J. Neurol. Sci.*, **279**, 26–29.
52. Association, A.D. (2009) Standards of medical care in diabetes--2009. *Diabetes Care*, **32**, S13–S61.

53. Kaneb, H.M., Sharp, P.S., Rahmani-Kondori, N. and Wells, D.J. (2011) Metformin treatment has no beneficial effect in a dose-response survival study in the SOD1(G93A) mouse model of ALS and is harmful in female mice. *PLoS ONE*, **6**, e24189.
54. Potenza, R.L., Armida, M., Ferrante, A., Pezzola, A., Matteucci, A., Puopolo, M. and Popoli, P. (2013) Effects of chronic caffeine intake in a mouse model of amyotrophic lateral sclerosis. *J. Neurosci. Res.*, **91**, 585–592.
55. Cashman, N.R., Durham, H.D., Blusztajn, J.K., Oda, K., Tabira, T., Shaw, I.T., Dahrouge, S. and Antel, J.P. (1992) Neuroblastoma x spinal cord (NSC) hybrid cell lines resemble developing motor neurons. *Dev. Dyn.*, **194**, 209–221.
56. Hylden, J.L. and Wilcox, G.L. (1980) Intrathecal morphine in mice: a new technique. *Eur. J. Pharm.*, **67**, 313–316.
57. Li, H.Y., Yeh, P.A., Chiu, H.C., Tang, C.Y. and Tu, B.P. (2011) Hyperphosphorylation as a defense mechanism to reduce TDP-43 aggregation. *PloS ONE*, **6**, e23075.
58. Chien, C.L., Wu, Y.S., Lai, H.L., Chen, Y.H., Jiang, S.T., Shih, C.M., Lin, S.S., Chang, C. and Chern, Y. (2010) Impaired water reabsorption in mice deficient in the type VI adenylyl cyclase (AC6). *FEBS Lett.*, **584**, 2883–2890.